Interaction Effect between Ellipsoidal Inclusions in an Infinite Body under Asymmetric Uniaxial Tension*

Nao-Aki NODA**, Kenji TOMARI***
and Tadatoshi MATSUO****

This paper deals with an interaction problem of two ellipsoidal inclusions under asymmetric uniaxial tension. The problem is solved on the superposition of two auxiliary loads; (i) biaxial tension and (ii) plane state of pure shear. These problems are formulated as a system of singular integral equations with Cauchy-type or logarithmic-type singularities, where the densities of the body forces distributed in the r, θ, z directions are unknown functions. In order to satisfy the boundary conditions along the boundaries, the unknown functions are approximated by a linear combination of fundamental density functions and polynomials. The present method is found to yield rapidly converging numerical results and smooth stress distributions along the boundaries. For hard inclusions ($E_I/E_M>1$), the interaction appears as a large compressive stress σ_n; however, the maximum tensile stress is almost independent of the interaction. For soft inclusions ($E_I/E_M<1$), the interaction appears as a large tensile stress σ_θ.

Key Words: Elasticity, Body Force Method, Numerical Analysis, Stress Concentration Factor, Ellipsoidal Inclusion

1. Introduction

Most engineering materials contain some defects in the form of cracks, voids, inclusions, or second-phased particles. To evaluate the effect of defects on the strength of structures, it is necessary to know the stress concentration of those defects. As a model of defects elliptical and ellipsoidal inclusions are important because they cover a wide variety of particular cases, such as line, circular, and spherical defects. In previous studies a single ellipsoidal inclusion, 2D elliptical inclusions, and 3D symmetric inclusion problems are treated by several authors[1]-[14]. However, few studies are made for 3D asymmetric problems except for spherical cavities under asymmetric uniaxial tension treated by Tsuchida[15],[16] et al. and ellipsoidal cavities treated by authors[17],[18].

This paper deals with an interaction problem of two ellipsoidal inclusions under asymmetric uniaxial tension on the idea of the body force method coupled with a singular integral equation formation. The problem is solved on the superposition of two auxiliary loads; (i) biaxial tension and (ii) plane state of pure shear. Then, the interaction effects will be discussed with varying the shape, spacing and elastic ratio of ellipsoidal inclusions.

2. Numerical Solutions

Consider an infinite body having two ellipsoidal inclusions under asymmetric uniaxial tension as shown in Fig. 1(c). This problem is composed of the superposition of Problems A and B as shown in Fig. 1. Rectangular and cylindrical coordinates (x, y, z) and

* Received 18th January, 1999. Japanese original: Trans. Jpn. Soc. Mech. Eng., Vol. 64, No. 622, A (1998), p. 1577-1582 (Received 29th March, 1998)
** Department of Mechanical Engineering, Kyushu Institute of Technology, 1-1 Sensuicho, Tobata Kitakyushu 804-8550, Japan. E-mail: noda@mech.kyutech.ac.jp
*** Graduate Student, Kyushu Institute of Technology, 1-1 Sensuicho, Tobata Kitakyushu 804-8550, Japan
**** Department of Mechanical Engineering, Fukushima National College of Technology, 30 Nagao, Kamiarakawa, Taira, Iwaki 970-8034, Japan

NII-Electronic Library Service

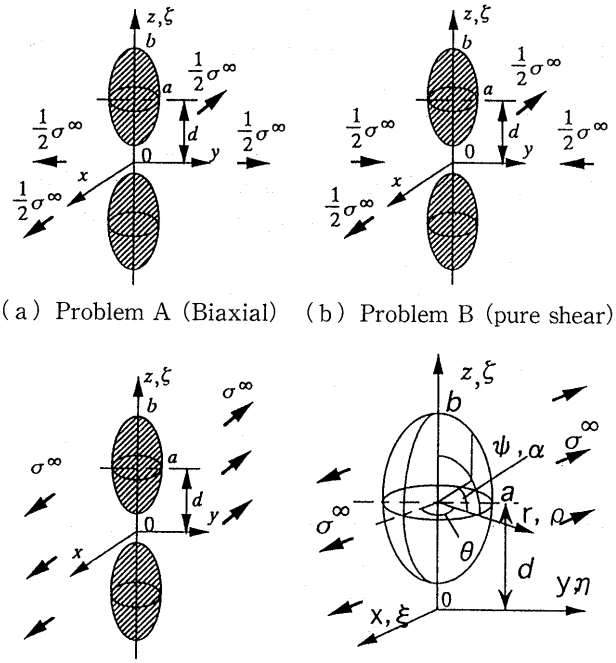

(a) Problem A (Biaxial) (b) Problem B (pure shear)

(c) Problem C (Uniaxial) (d) Coordinate system

Fig. 1 Problem and coordinate system

(r, θ, z) are defined as shown in Fig. 1. Here, (ξ, η, ζ) and (ρ, ϕ, ζ) are rectangular and cylindrical coordinates that specify the points where body forces are distributed. The problem A can be analyzed by applying the solution described in our previous paper[14]. In this paper, therefore, the solution of the problem B will be mainly explained.

First, the body force method is used to formulate the problem as a system of singular integral equations. Here, the fundamental solutions are stress $(K_{nn}^{Fr}, K_{nn}^{F\theta}, \cdots\cdots, K_{nt}^{F\theta}, K_{nt}^{Fz})$ and displacement fields $(K_{ur}^{Fr}, K_{ur}^{F\theta}, \cdots\cdots, K_{uz}^{F\theta}, K_{uz}^{Fz})$ at an arbitrary point $(r=a\cos\psi, z=d+b\sin\psi)$ when two ring forces acting symmetrically to the plane $z=0$. In this case we should consider the boundary condition only on $z\geqq 0$ because the problem B is symmetric with respect to $z=0$. Here, it should be noted that each ring force has the magnitude proportional to $\cos 2\phi$ or $\sin 2\phi$ along the circumference[17]-[20]. Then, the problem can be formulated in terms of singular integral equations by using the fundamental solutions due to ring forces in two infinite bodies "M" and "I". Here, the infinite body "M" has the same elastic constants as those of the matrix (E_M, ν_M) and the infinite body "I" has the same ones as those of the inclusions (E_I, ν_I). The integral equations are expressed in Eqs.(1)-(6), where unknowns are the body force densities distributed in the infinite body M and I in the r, θ, z directions along the circumference specified by the angle α $\rho_{rM}^*(\alpha)$, $\rho_{\theta M}^*(\alpha)$, $\rho_{zM}^*(\alpha)$, $\rho_{rI}^*(\alpha)$, $\rho_{\theta I}^*(\alpha)$, $\rho_{zI}^*(\alpha)$.

$$
\begin{aligned}
&-1/2\{\rho_{rM}^*(\psi)\cos\psi_0+\rho_{zM}^*(\psi)\sin\psi_0\}\\
&-1/2\{\rho_{rI}^*(\psi)\cos\psi_0+\rho_{zI}^*(\psi)\sin\psi_0\}\\
&+\int_{-\pi/2}^{\pi/2}K_{nnM}^{Fr}(\alpha,\psi)\rho_{rM}^*(\alpha)ds\\
&+\int_{-\pi/2}^{\pi/2}K_{nnM}^{F\theta}(\alpha,\psi)\rho_{\theta M}^*(\alpha)ds\\
&+\int_{-\pi/2}^{\pi/2}K_{nnM}^{Fz}(\alpha,\psi)\rho_{zM}^*(\alpha)ds\\
&-\int_{-\pi/2}^{\pi/2}K_{nnI}^{Fr}(\alpha,\psi)\rho_{rI}^*(\alpha)ds\\
&-\int_{-\pi/2}^{\pi/2}K_{nnI}^{F\theta}(\alpha,\psi)\rho_{\theta I}^*(\alpha)ds\\
&-\int_{-\pi/2}^{\pi/2}K_{nnI}^{Fz}(\alpha,\psi)\rho_{zI}^*(\alpha)ds\\
&=-\sigma_r^\infty\cos^2\psi_0\cos 2\theta \qquad (1)\\
&-1/2\{\rho_{\theta M}^*(\psi)+\rho_{\theta I}^*(\psi)\}\\
&+\int_{-\pi/2}^{\pi/2}K_{n\theta M}^{Fr}(\alpha,\psi)\rho_{rM}^*(\alpha)ds\\
&+\int_{-\pi/2}^{\pi/2}K_{n\theta M}^{F\theta}(\alpha,\psi)\rho_{\theta M}^*(\alpha)ds\\
&+\int_{-\pi/2}^{\pi/2}K_{n\theta M}^{Fz}(\alpha,\psi)\rho_{zM}^*(\alpha)ds\\
&-\int_{-\pi/2}^{\pi/2}K_{n\theta I}^{Fr}(\alpha,\psi)\rho_{rI}^*(\alpha)ds\\
&-\int_{-\pi/2}^{\pi/2}K_{n\theta I}^{F\theta}(\alpha,\psi)\rho_{\theta I}^*(\alpha)ds\\
&-\int_{-\pi/2}^{\pi/2}K_{n\theta I}^{Fz}(\alpha,\psi)\rho_{zI}^*(\alpha)ds\\
&=-\tau_{r\theta}^\infty\cos\psi_0\sin 2\theta \qquad (2)\\
&-1/2\{-\rho_{rM}^*(\psi)\sin\psi_0+\rho_{zM}^*(\psi)\cos\psi_0\}\\
&-1/2\{-\rho_{rI}^*(\psi)\sin\psi_0+\rho_{zI}^*(\psi)\cos\psi_0\}\\
&+\int_{-\pi/2}^{\pi/2}K_{ntM}^{Fr}(\alpha,\psi)\rho_{rM}^*(\alpha)ds\\
&+\int_{-\pi/2}^{\pi/2}K_{ntM}^{F\theta}(\alpha,\psi)\rho_{\theta M}^*(\alpha)ds\\
&+\int_{-\pi/2}^{\pi/2}K_{ntM}^{Fz}(\alpha,\psi)\rho_{zM}^*(\alpha)ds\\
&-\int_{-\pi/2}^{\pi/2}K_{ntI}^{Fr}(\alpha,\psi)\rho_{rI}^*(\alpha)ds\\
&-\int_{-\pi/2}^{\pi/2}K_{ntI}^{F\theta}(\alpha,\psi)\rho_{\theta I}^*(\alpha)ds\\
&-\int_{-\pi/2}^{\pi/2}K_{ntI}^{Fz}(\alpha,\psi)\rho_{zI}^*(\alpha)ds\\
&=-\sigma_r^\infty\sin\psi_0\cos\psi_0\cos 2\theta \qquad (3)\\
&\int_{-\pi/2}^{\pi/2}K_{urM}^{Fr}(\alpha,\psi)\rho_{rM}^*(\alpha)ds+\int_{-\pi/2}^{\pi/2}K_{urM}^{F\theta}(\alpha,\psi)\rho_{\theta M}^*(\alpha)ds\\
&+\int_{-\pi/2}^{\pi/2}K_{urM}^{Fz}(\alpha,\psi)\rho_{zM}^*(\alpha)ds\\
&-\int_{-\pi/2}^{\pi/2}K_{urI}^{Fr}(\alpha,\psi)\rho_{rI}^*(\alpha)ds\\
&-\int_{-\pi/2}^{\pi/2}K_{urI}^{F\theta}(\alpha,\psi)\rho_{\theta I}^*(\alpha)ds\\
&-\int_{-\pi/2}^{\pi/2}K_{urI}^{Fz}(\alpha,\psi)\rho_{zI}^*(\alpha)ds\\
&=-(\sigma_r^\infty-\nu_M\sigma_\theta^\infty)r/E_M\cos 2\theta \qquad (4)\\
&\int_{-\pi/2}^{\pi/2}K_{u\theta M}^{Fr}(\alpha,\psi)\rho_{rM}^*(\alpha)ds+\int_{-\pi/2}^{\pi/2}K_{u\theta M}^{F\theta}(\alpha,\psi)\rho_{\theta M}^*(\alpha)ds\\
&+\int_{-\pi/2}^{\pi/2}K_{u\theta M}^{Fz}(\alpha,\psi)\rho_{zM}^*(\alpha)ds\\
&-\int_{-\pi/2}^{\pi/2}K_{u\theta I}^{Fr}(\alpha,\psi)\rho_{rI}^*(\alpha)ds
\end{aligned}
$$

NII-Electronic Library Service

$$-\int_{-\pi/2}^{\pi/2} K_{u\theta I}^{F\theta}(\alpha,\psi)\rho_{\theta I}^{*}(\alpha)ds$$
$$-\int_{-\pi/2}^{\pi/2} K_{uzI}^{Fz}(\alpha,\psi)\rho_{zI}^{*}(\alpha)ds$$
$$=-\tau_{r\theta}^{\infty}2(1+\nu_M)r/E_M\sin 2\theta \qquad (5)$$

$$\int_{-\pi/2}^{\pi/2} K_{uzM}^{Fr}(\alpha,\psi)\rho_{rM}^{*}(\alpha)ds+\int_{-\pi/2}^{\pi/2} K_{uzM}^{F\theta}(\alpha,\psi)\rho_{\theta M}^{*}(\alpha)ds$$
$$+\int_{-\pi/2}^{\pi/2} K_{uzM}^{Fz}(\alpha,\psi)\rho_{zM}^{*}(\alpha)ds$$
$$-\int_{-\pi/2}^{\pi/2} K_{uzI}^{Fr}(\alpha,\psi)\rho_{rI}^{*}(\alpha)ds$$
$$-\int_{-\pi/2}^{\pi/2} K_{uzI}^{F\theta}(\alpha,\psi)\rho_{\theta I}^{*}(\alpha)ds$$
$$-\int_{-\pi/2}^{\pi/2} K_{uzI}^{Fz}(\alpha,\psi)\rho_{zI}^{*}(\alpha)ds$$
$$=-\nu_M(\sigma_r^{\infty}+\sigma_\theta^{\infty})z/E_M\cos 2\theta \qquad (6)$$

where

$$-d\rho=a\sin\alpha d\alpha,\ d\zeta=b\cos\alpha d\alpha,$$
$$ds=\sqrt{a^2\sin^2\alpha+b^2\cos^2\alpha}\,d\alpha \qquad (7)$$

Here ψ_0 is the angle between the r-axis and the normal direction of ellipsoidal inclusion at (r, z). The unknown functions in Eqs.(1)-(6) $\rho_{rM}^{*}(\alpha)$, $\rho_{\theta M}^{*}(\alpha)$, $\rho_{zM}^{*}(\alpha)$ are defined by the following equations. Other unknown functions $\rho_{rI}^{*}(\alpha)$, $\rho_{\theta I}^{*}(\alpha)$, $\rho_{zI}^{*}(\alpha)$ can be expressed in a similar way.

$$\rho_{rM}^{*}(\alpha)\cos 2\varphi=\frac{dF_r}{\rho d\phi ds},\ \rho_{\theta M}^{*}(\alpha)\sin 2\varphi=\frac{dF_\theta}{\rho d\phi ds},$$
$$\rho_{zM}^{*}(\alpha)\cos 2\varphi=\frac{-dF_z}{\rho d\phi ds} \qquad (8)$$

Here dF_r, dF_θ, dF_z are the components of the resultant of the body force in the r, θ, z directions, respectively, acting on the infinitesimal area $rd\phi ds$. Equations (1)-(6) enforce boundary conditions at the imaginary boundary; that is, $\sigma_{nM}-\sigma_{nI}=0$, $\tau_{n\theta M}-\tau_{n\theta I}=0$, $\tau_{ntM}-\tau_{ntI}=0$, $u_{rM}-u_{rI}=0$, $u_{\theta M}-u_{\theta I}=0$, $u_{zM}-u_{zI}=0$. Equations (1)-(3) include the Cauchy-type singularity and Eqs.(4)-(6) include the logarithmic-type singularity. Therefore in Eqs.(1)-(3), the integration should be interpreted as a meaning of Cauchy principal value.

As shown in Eqs.(1)-(6), the problem is reduced to determining the body force densities $\rho_{rM}^{*}(\alpha)\sim\rho_{zI}^{*}(\alpha)$. In the present method, auxiliary functions $[f_1(\alpha), f_2(\alpha)]$, which are defined by original unknown functions, will be determined instead of determining the original functions directly. In the following equations, the notation $f(\alpha)$ means the original unknowns $\rho_{rM}^{*}(\alpha)\sim\rho_{zI}^{*}(\alpha)$, and $f_1(\alpha), f_2(\alpha)$, means the auxiliary functions obtained from $f(\alpha)$ as shown in Eq.(9).

$$f_1(\alpha)=\{f(\alpha)+f(-\alpha)\}/2,\ f_2(\alpha)=\{f(\alpha)-f(-\alpha)\}/2 \qquad (9)$$

Here, $f_1(\alpha), f_2(\alpha)$ satisfy following equations.

$$f_1(\alpha)=f_1(-\alpha),\ f_2(\alpha)=-f_2(-\alpha) \qquad (10)$$

Determining auxiliary functions $f_1(\alpha), f_2(\alpha)$ in the range $0\leqq\alpha\leqq\pi/2$ is equivalent to determining the unknown functions $f(\alpha)$ in the range $-\pi/2\leqq\alpha\leqq\pi/2$. In other words, if the auxiliary functions are given in the range $0\leqq\alpha\leqq\pi/2$, the original unknown functions $f(\alpha)$ are expressed in the range $-\pi/2\leqq\alpha\leqq\pi/2$.

$$f(\alpha)=f_1(\alpha)+f_2(\alpha)$$
$$f(-\alpha)=f_1(-\alpha)-f_2(-\alpha)=f_1(\alpha)-f_2(\alpha) \qquad (11)$$

Then, fundamental density functions are defined as continuous functions satisfying Eq.(10) as follows:

$$w_{r3}(\alpha)=w_{\theta 3}(\alpha)=n_r(\alpha),$$
$$w_{r4}(\alpha)=w_{\theta 4}(\alpha)=n_r(\alpha)\sin(\alpha),$$
$$w_{z1}(\alpha)=n_z(\alpha)/\sin(\alpha),\ w_{z2}(\alpha)=n_z(\alpha) \qquad (12)$$
$$n_r(\alpha)=\frac{b\cos\alpha}{\sqrt{a^2\sin^2\alpha+b^2\cos^2\alpha}},$$
$$n_z(\alpha)=\frac{a\sin\alpha}{\sqrt{a^2\sin^2\alpha+b^2\cos^2\alpha}} \qquad (13)$$

Here, $w_{r3}(\alpha)$, $w_{\theta 3}(\alpha)$, $w_{z1}(\alpha)$ satisfy the first Eq.(10) and $w_{r4}(\alpha)$, $w_{\theta 4}(\alpha)$, $w_{z2}(\alpha)$ satisfy the second Eq.(10). Here, it should be noted that $w_{r3}(\alpha)$, $w_{\theta 3}(\alpha)$, $w_{z2}(\alpha)$ are exact densities of body force to express a single ellipsoidal inclusion under plane state of pure shear.

The unknown functions $\rho_{rM}^{*}(\alpha)\sim\rho_{zI}^{*}(\alpha)$ can be expressed as a linear combination of the fundamental density functions and weight functions as shown in following equations.

$$\rho_{rM}^{*}(\alpha)=\rho_{r3M}(\alpha)w_{r3}(\alpha)+\rho_{r4M}(\alpha)w_{r4}(\alpha)$$
$$\rho_{\theta M}^{*}(\alpha)=\rho_{\theta 3M}(\alpha)w_{\theta 3}(\alpha)+\rho_{\theta 4M}(\alpha)w_{\theta 4}(\alpha)$$
$$\rho_{zM}^{*}(\alpha)=\rho_{z2M}(\alpha)w_{z2}(\alpha)+\rho_{z1M}(\alpha)w_{z1}(\alpha)$$
$$\rho_{rI}^{*}(\alpha)=\rho_{r3I}(\alpha)w_{r3}(\alpha)+\rho_{r4I}(\alpha)w_{r4}(\alpha)$$
$$\rho_{\theta I}^{*}(\alpha)=\rho_{\theta 3I}(\alpha)w_{\theta 3}(\alpha)+\rho_{\theta 4I}(\alpha)w_{\theta 4}(\alpha)$$
$$\rho_{zI}^{*}(\alpha)=\rho_{z2I}(\alpha)w_{z2}(\alpha)+\rho_{z1I}(\alpha)w_{z1}(\alpha) \qquad (14)$$

In Eqs.(14), taking $\rho_{rM}^{*}(\alpha)$ for example, $\rho_{r3M}(\alpha)w_{r3}(\alpha)$ correspond to $f_1(\alpha)$ of Eq.(11) and $\rho_{r4M}^{*}(\alpha)w_{r4}(\alpha)$ correspond to $f_2(\alpha)$ of Eq.(11). Then, all weight functions $\rho_{r3M}(\alpha), \cdots, \rho_{z1I}(\alpha)$ must satisfy Eq.(15).

$$g(\alpha)=g(-\alpha) \qquad (15)$$

where $g(\alpha)$ means the weight functions $\rho_{r3M}(\alpha), \cdots, \rho_{z1I}(\alpha)$. In problem B, the following equations have been applied.

$$\rho_{r3M}(\alpha)=\sum_{n=1}^{M/2}a_{nM}t_n(\alpha),\ \rho_{r4M}(\alpha)=\sum_{n=1}^{M/2}b_{nM}t_n(\alpha),$$
$$\rho_{\theta 3M}(\alpha)=\sum_{n=1}^{M/2}c_{nM}t_n(\alpha),\ \rho_{\theta 4M}(\alpha)=\sum_{n=1}^{M/2}d_{nM}t_n(\alpha),$$
$$\rho_{z2M}(\alpha)=\sum_{n=1}^{M/2}e_{nM}t_n(\alpha),\ \rho_{z1M}(\alpha)=\sum_{n=1}^{M/2}f_{nM}t_n(\alpha),$$
$$\rho_{r3I}(\alpha)=\sum_{n=1}^{M/2}a_{nI}t_n(\alpha),\ \rho_{r4I}(\alpha)=\sum_{n=1}^{M/2}b_{nI}t_n(\alpha),$$
$$\rho_{\theta 3I}(\alpha)=\sum_{n=1}^{M/2}c_{nM}t_n(\alpha),\ \rho_{\theta 4I}(\alpha)=\sum_{n=1}^{M/2}d_{nI}t_n(\alpha),$$
$$\rho_{z2I}(\alpha)=\sum_{n=1}^{M/2}e_{nI}t_n(\alpha),\ \rho_{z1I}(\alpha)=\sum_{n=1}^{M/2}f_{nI}t_n(\alpha) \qquad (16)$$

$$t_n(\alpha)=\cos\{2(n-1)\alpha\} \qquad (17)$$

where M is the number of the collocation points in $-\pi/2\leqq\alpha\leqq\pi/2$. Here, Eq.(15) is always satisfied for all the weight functions $\rho_{r3M}(\alpha), \cdots, \rho_{z1I}(\alpha)$ when the

NII-Electronic Library Service

Eqs. (16), (17) are used.

Using the approximation method mentioned above, the singular integral equations are reduced to a system of algebraic equations for determining the coefficients $a_{nM}, b_{nM}, \cdots, f_{nI}$. The number of coefficients is $4M$. Using the numerical solution mentioned above we will obtain the stress distribution along the interface and discuss the maximum stress.

Table 1 Convergence of unknown function (Problem B, $a/b=1.0$, $b/d=0.8$, $E_I/E_M=10^5$)

Ψ	M	ρ_{r3M}	$\rho_{\theta 3M}$	ρ_{Z2M}	ρ_{r4M}	$\rho_{\theta 4M}$	ρ_{Z1M}
0	12	-2.0455	-2.0602	-0.0770	-0.0919	-0.0565	0.0364
	16	-2.0452	-2.0601	-0.0764	-0.0917	-0.0566	0.0360
	20	-2.0455	-2.0601	-0.0760	-0.0917	-0.0566	0.0360
10	12	-2.0422	-2.0581	-0.0781	-0.0947	-0.0585	0.0380
	16	-2.0422	-2.0582	-0.0778	-0.0945	-0.0586	0.0381
	20	-2.0427	-2.0581	-0.0779	-0.0946	-0.0586	0.0381
30	12	-2.0148	-2.0395	-0.0867	-0.1187	-0.0771	0.0542
	16	-2.0147	-2.0393	-0.0867	-0.1188	-0.0772	0.0541
	20	-2.0147	-2.0395	-0.0868	-0.1188	-0.0772	0.0541
60	12	-1.8962	-1.9284	-0.0736	-0.2165	-0.1801	0.0659
	16	-1.8960	-1.9282	-0.0736	-0.2167	-0.1803	0.0658
	20	-1.8960	-1.9282	-0.0736	-0.2167	-0.1803	0.0658
80	12	-1.7829	-1.7894	-0.0143	-0.3075	-0.3009	0.0140
	16	-1.7830	-1.7895	-0.0140	-0.3074	-0.3009	0.0140
	20	-1.7830	-1.7895	-0.0140	-0.3074	-0.3009	0.0140
90	12	-1.7608	-1.7607	-0.0000	-0.3251	-0.3253	0.0000
	16	-1.7606	-1.7606	-0.0000	-0.3254	-0.3254	0.0000
	20	-1.7605	-1.7605	-0.0000	-0.3255	-0.3254	0.0000

Table 2 Maximum stress of two spherical cavities ($a/b=1.0$, $E_I/E_M=0$)

a/d	(deg.)	$\sigma_{\theta max}$	$\sigma_{\theta A}$	$\sigma_{\theta B}$
0	-90~+90 (-90~+90)	2.0455 (2.045)	2.0455 (2.045)	2.0455 (2.045)
0.1	-2 (0)	2.0455 (2.046)	2.0450 (2.045)	2.0450 (2.045)
0.2	-10 (-10)	2.0462 (2.046)	2.0433 (2.045)	2.0433 (2.045)
0.3	-10 (-15)	2.0481 (2.048)	2.0423 (2.043)	2.0452 (2.046)
0.4	-17 (-20)	2.0508 (2.052)	2.0375 (2.038)	2.0460 (2.046)
0.5	-25 (-25)	2.0599 (2.060)	2.0304 (2.031)	2.0478 (2.048)
0.6	-31 (-30)	2.0742 (2.074)	2.0292 (2.029)	2.0509 (2.051)
0.7	-41	2.1022	2.0652	2.0557
0.8	-90 (-90)	2.2296 (2.230)	2.2296 (2.230)	2.0620 (2.062)
0.9	-90	2.7741	2.7741	2.0701

( ) : Tsuchida[15]

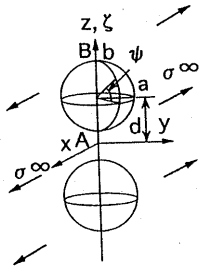

3. Numerical Results and Discussion

3.1 Convergence of the results

Table 1 shows the convergence of unknown functions $\rho_{r3M}(\alpha)$, $\rho_{\theta 3M}(\alpha)$, $\rho_{z2M}(\alpha)$, $\rho_{r3I}(\alpha)$, $\rho_{\theta 3I}(\alpha)$, $\rho_{z2I}(\alpha)$ with increasing the collocation number M when $a/b=1.0$, $b/d=0.8$, $E_I/E_M=10^5$ for problem B in Fig. 1. The present results have shown good convergence to the fifth digit when $M=20$. Also the boundary conditions are confirmed to be less than 10^{-4} for $\sigma_{nM}-\sigma_{nI}$, $\tau_{n\theta M}-\tau_{n\theta I}$, $\tau_{ntM}-\tau_{ntI}$, $u_{rM}-u_{rI}$, $u_{\theta M}-u_{\theta I}$, $u_{zM}-u_{zI}$. The present method yields rapidly converging results and highly satisfied boundary conditions.

3.2 Results of ellipsoidal cavities

First of all, results of cavities ($E_I/E_M=0$) will be shown. Table 2 indicates the maximum stresses with their positions and the stresses at points A and B for

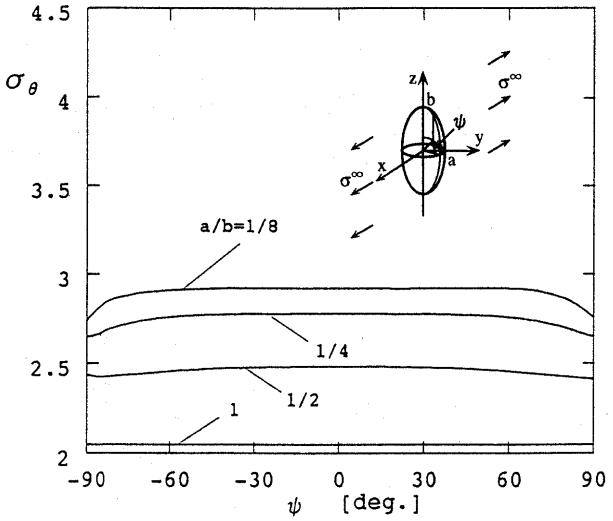

Fig. 2 Boundary stress σ_θ for a single cavity on $\theta=\pi/2$ ($E_I/E_M=0$, $b/d=0$)

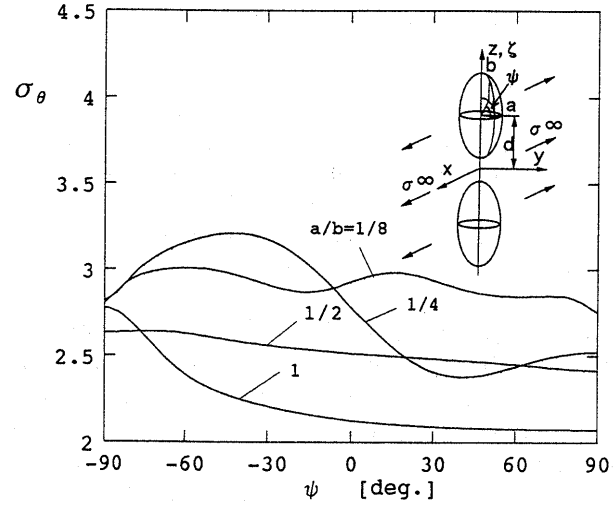

Fig. 3 Boundary stress σ_θ on $\theta=\pi/2$ ($E_I/E_M=0$, $b/d=0.9$)

NII-Electronic Library Service

Table 3 Maximum stress of two ellipsoidal cavities ($E_I/E_M=0$)

b/d	0		1/3		1/2		2/3		0.8		0.9	
a/b	(deg.)	σ_θ	(deg.)	σ_θ	(deg.)	σ_θ	(deg.)	σ_θ	(deg.)	σ_θ	(deg.)	σ_θ
1	-90-90	2.0454	-17	2.0492	-25	2.0599	-37	2.0905	-90	2.2296	-90	2.7741
1/2	0	2.4084	-1	2.4814	-7	2.4846	-24	2.4938	-47	2.5240	-72	2.6363
1/4	0	2.7772	-12	2.7780	-28	2.7859	-37	2.8221	-39	2.9246	-42	3.2051
1/8	0	2.9235	15	2.9243	20	2.9218	-51	2.9258	-56	2.9478	-59	3.0044

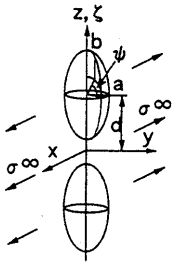

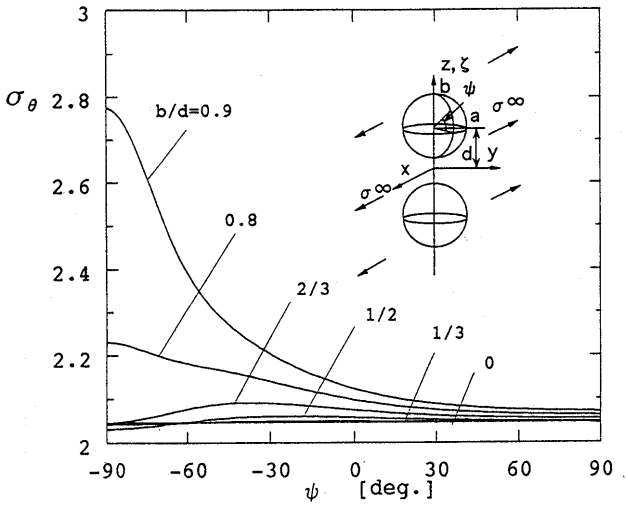

Fig. 4 Boundary stress σ_θ on $\theta=\pi/2$ ($E_I/E_M=0$, $a/b=1.0$)

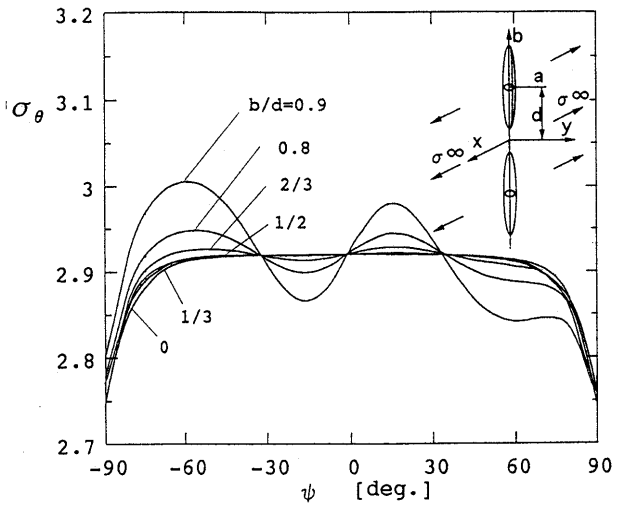

Fig. 5 Boundary stress σ_θ on $\theta=\pi/2$ ($E_I/E_M=0$, $a/b=1/8$)

spherical cavities ($a/b=1.0$). Tuchida's results coincide with the present results to the fourth digit in most cases. Figure 2 shows boundary stress of a single cavity ($b/d=0$), and Fig. 3 shows boundary stress when $b/d=0.9$. When $a/b=1$ and 1/2, the interaction is large near $\psi=-\pi/2$; on the other hand, when $a/b=$ 1/4 and 1/8, the interaction appears in a different way. Figures 4 and 5 show boundary stresses when $a/b=$

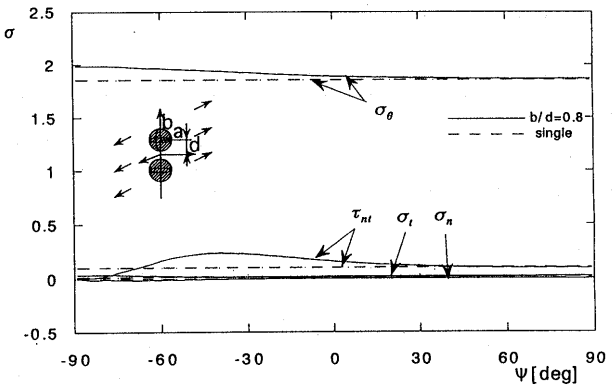

Fig. 6 Interface stresses σ_n, σ_θ, σ_t, τ_{nt}, σ_1 on $\theta=0$ and $\tau_{n\theta}$ on $\theta=\pi/4$ ($a/b=1.0$, $E_I/E_M=10^5$)

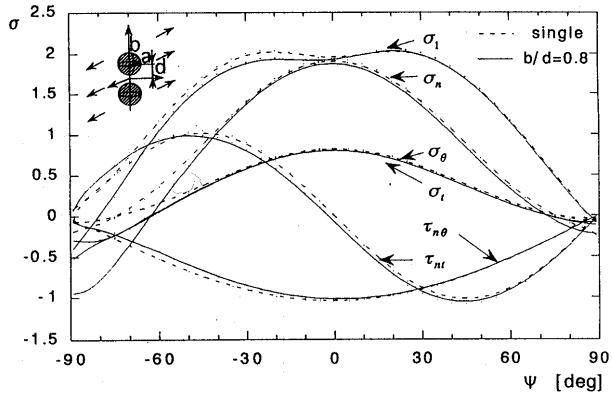

Fig. 7 Interface stresses σ_n, σ_θ, σ_t, τ_{nt} on $\theta=0$ ($a/b=1.0$, $E_I/E_M=0.1$)

1.0, 1/8. Maximum stresses and their positions are shown in Table 3.

3.3 Results of a single inclusion

Figure 6 shows interface stresses of spherical inclusions when $a/b=1.0$ and $E_I/E_M=10^5$. The solid lines for $a/d=0.8$ are compared with the broken lines for a single inclusion ($a/d=0$). In Fig. 6, stress distributions are shown on the plane $\theta=0$ except for $\tau_{n\theta}$ on the plane $\theta=\pi/4$. The notation σ_1 means maximum principal stress that is obtained from σ_n, σ_t, σ_{nt}. The interaction mainly appears as a compressive stress σ_n around $\psi=-\pi/2$.

Figure 7 shows interface stresses on $\theta=\pi/2$ of spherical inclusions when $a/b=1.0$ and $E_I/E_M=0.1$. The stress σ_θ is larger than others and the interaction

NII-Electronic Library Service

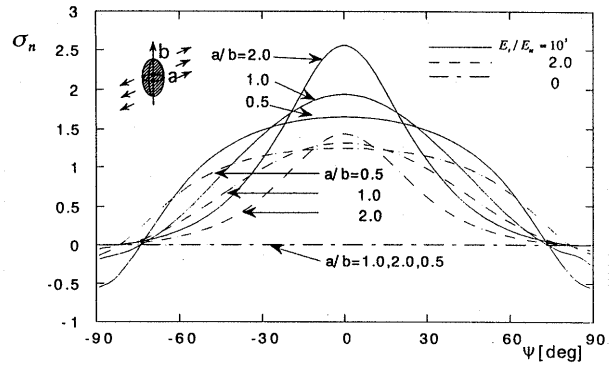

Fig. 8 Interface stress σ_n on $\theta=0$ ($a/b=0.5, 1.0, 2.0$, $E_I/E_M=10^5, 2.0, 0$)

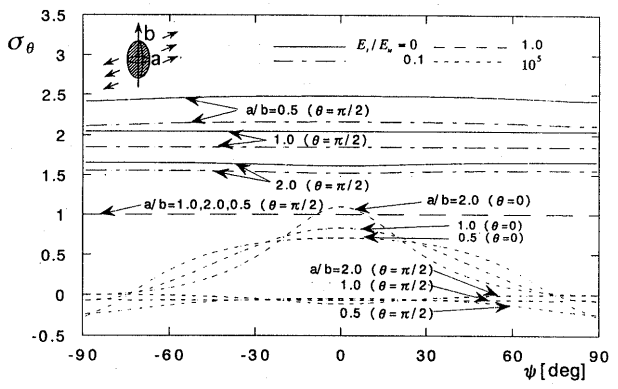

Fig. 9 Interface stress σ_θ on $\theta=\pi/2$ ($a/b=0.5, 1.0, 2.0$, $E_I/E_M=10^5, 1.0, 0.1, 0$)

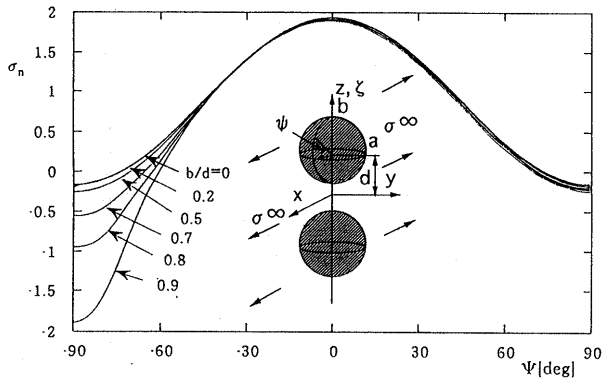

Fig. 10 Interface stress σ_n on $\theta=0$ ($a/b=1.0$, $E_I/E_M=10^5$)

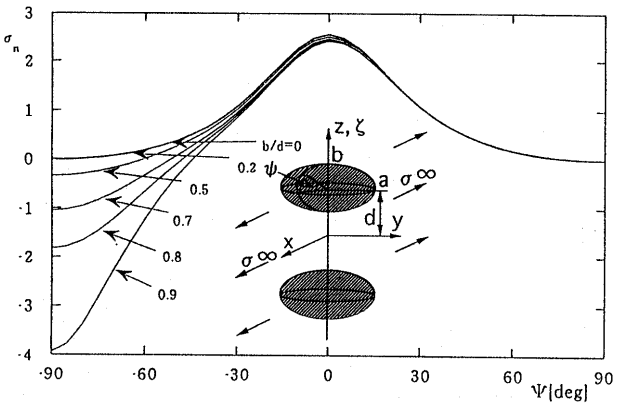

Fig. 11 Interface stress σ_n on $\theta=0$ ($a/b=2.0$, $E_I/E_M=10^5$)

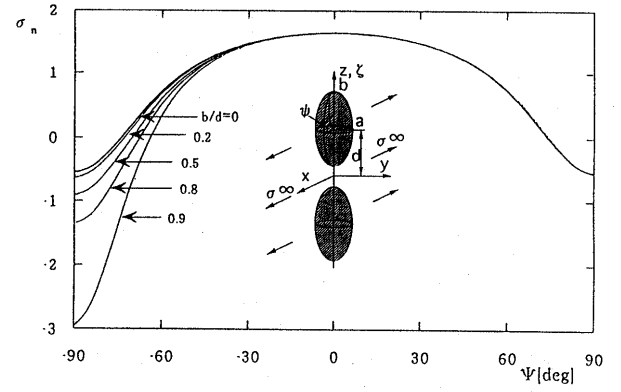

Fig. 12 Interface stress σ_n on $\theta=0$ ($a/b=0.5$, $E_I/E_M=10^5$)

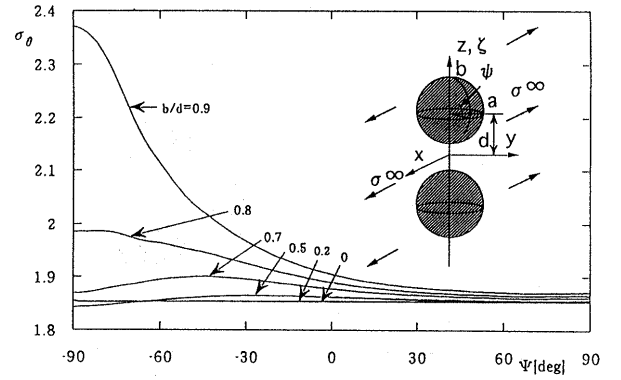

Fig. 13 Interface stress σ_θ on $\theta=\pi/2$ ($a/b=1.0$, $E_I/E_M=0.1$)

of σ_θ appears around $\psi=-\pi/2$. From Figs. 6 and 7, we will mainly discuss the interaction for σ_n on $\theta=0$ when $E_I/E_M>1$ and for σ_θ on $\theta=\pi/2$ when $E_I/E_M<1$.

Figure 8 shows an interface stress σ_n on $\theta=0$, and Fig. 9 shows σ_θ on $\theta=\pi/2$, both for a single ellipsoidal inclusion. When $E_I/E_M=10^5$, σ_θ on $\theta=0$ is also shown in Fig. 9 because the value is larger than the one on $\theta=\pi/2$. For a single inclusion we can see the maximum stresses for different E_I/E_M. In following section, the interaction will be discussed by taking example of $E_I/E_M=10^5$ and $E_I/E_M=0.1$.

3.4 Results of two ellipsoidal inclusions

Figures 10, 11, 12 show the interface stress σ_n when $a/b=1$, 2.0, 0.5, respectively. The interaction appears near $\psi=-\pi/2$ as a large compressive stress especially when $b/d>0.7$. However, the maximum tensile stress σ_n near $\psi=0$, which may cause debonding the interface, is almost independent of the interaction. On the other hand, when $E_I/E_M=0.1$ as shown in Figs. 13-15, the interaction appears as a large tensile stress σ_θ similarly to the case of cavities ($E_I/E_M=0$). When b/d and E_I/E_M are fixed, the interaction appears largely when a/b is large in Figs. 10-15.

Tables 4-6 show maximum stresses σ_n and σ_θ and their positions. The maximum stress appears near $\psi=0$ when $E_I/E_M=10, 10^5$. Then, the interaction

NII-Electronic Library Service

Table 4 Maximum stress of two ellipsoidal inclusions ($a/b=1.0$)

a/b=1.0		Matrix			
E_I/E_M	b/d	ψ (deg)	σ_n	ψ (deg)	σ_θ
		$\theta=\pi/2$			
0	0			-90~90	2.0455
	0.2			-90	2.0462
	0.5			-25	2.0599
	0.7			-90	2.1569
	0.8			-90	2.2302
	0.9			-90	2.7773
		$\theta=0$		$\theta=\pi/2$	
0.1	0	0	0.1919	-90~90	1.8540
	0.2	0	0.1920	-90~90	1.8546
	0.5	0	0.1931	-25	1.8643
	0.7	0	0.1955	-45	1.8956
	0.8	0	0.1972	-90	1.9931
	0.9	0	0.1992	-90	2.3860
		$\theta=0$		$\theta=0$	
10	0	0	1.7684	0	0.6698
	0.2	0	1.7682	0	0.6697
	0.5	0	1.7627	0	0.6681
	0.7	0	1.7492	0	0.6636
	0.8	0	1.7386	0	0.6602
	0.9	0	1.7261	0	0.6561
		$\theta=0$		$\theta=0$	
10^5	0	0	1.9383	0	0.8307
	0.2	0	1.9381	0	0.8306
	0.5	0	1.9316	0	0.8278
	0.7	0	1.9155	0	0.8208
	0.8	0	1.9033	0	0.8156
		(-90)	(-0.9528)	(-90)	(-0.4083)
	0.9	0	1.8887	0	0.8094
		(-90)	(-1.9132)	(-90)	(-0.8198)

Table 5 Maximum stress of two ellipsoidal inclusions ($a/b=2.0$)

a/b=2.0		Matrix			
E_I/E_M	b/d	ψ (deg)	σ_n	ψ (deg)	σ_θ
				$\theta=\pi/2$	
0	0			±90	1.6601
	0.2			90	1.6595
	0.5			-32	1.6748
	0.7			-90	1.8863
	0.8			-90	2.1725
	0.9			-90	2.7818
		$\theta=0$		$\theta=\pi/2$	
0.1	0	0	0.1559	±85	1.5565
	0.2	0	0.1562	90	1.5565
	0.5	0	0.1599	-36	1.5699
	0.7	1	0.1621	-90	1.7363
	0.8	1	0.1623	-90	1.9502
	0.9	1	0.1636	-90	2.3688
		$\theta=0$		$\theta=0$	
10	0	0	2.2084	0	0.8337
	0.2	0	2.2074	0	0.8335
	0.5	1	2.1817	0	0.8272
	0.7	1	2.1490	0	0.8171
	0.8	1	2.1331	0	0.8133
	0.9	1	2.1190	0	0.8102
				(-90)	(-0.9700)
		$\theta=0$		$\theta=0$	
10^5	0	0	2.5575	0	1.0961
	0.2	0	2.5558	0	1.0951
	0.5	0	2.5152	0	1.0766
	0.7	0	2.4613	0	1.0533
	0.8	1	2.4352	0	1.0432
		(-90)	(-1.8246)	(-90)	(-0.7611)
	0.9	1	2.4154	0	1.0326
		(-90)	(-3.9027)	(-90)	(-1.6664)

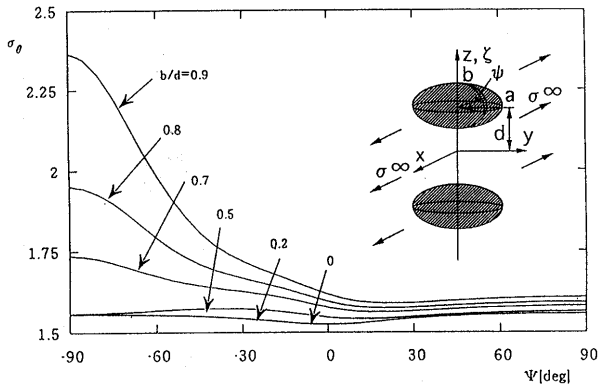

Fig. 14 Interface stress σ_θ on $\theta=\pi/2$ ($a/b=2.0$, $E_I/E_M=0.1$)

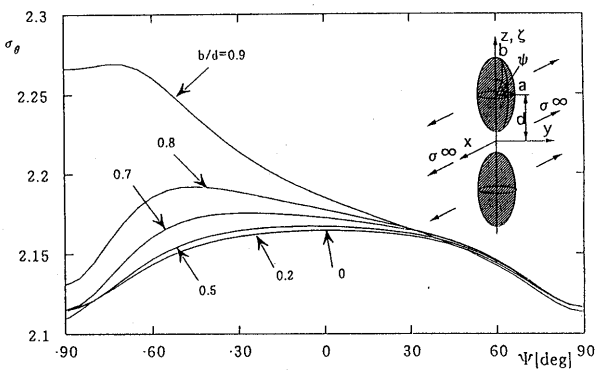

Fig. 15 Interface stress σ_θ on $\theta=\pi/2$ ($a/b=0.5$, $E_I/E_M=0.1$)

appears as a large compressive stress when b/d becomes large at $\psi=-\pi/2$. The position of maximum stress varies depending on b/d when $E_I/E_M=0, 0.1$.

4. Conclusion

In this study, two ellipsoidal inclusions in an infinite body under asymmetric uniaxial tension are considered using singular integral equations of the body force method. The conclusion can be made as follows.

(1) The problem is solved on the superposition of two auxiliary loads; (i) biaxial tension and (ii) plane state of pure shear. In order to satisfy the boundary conditions, the unknown functions are approximated by a linear combination of fundamental density functions and polynomials. The present method is found to yields rapidly converging numerical results and smooth stress distribution along the boundary.

(2) The maximum stresses and interface stresses are shown in tables and figures for various shape, spacing, and elastic ratio of inclusions. Tuchida's results for spheroidal cavities coincide with the present results to the fourth digit in most cases.

NII-Electronic Library Service

Table 6 Maximum stress of two ellipsoidal inclusions ($a/b=0.5$)

a/b=0.5		Matrix			
E_I/E_M	b/d	ψ (deg)	σ_n	ψ (deg)	σ_θ
				$\theta=\pi/2$	
0	0			0	2.4804
	0.2			0	2.4806
	0.5			-7	2.4846
	0.7			-30	2.4979
	0.8			-47	2.5240
	0.9			-73	2.6363
		$\theta=0$		$\theta=\pi/2$	
0.1	0	0	0.2246	0	2.1643
	0.2	0	0.2247	0	2.1644
	0.5	0	0.2249	-5	2.1671
	0.7	0	0.2256	-28	2.1755
	0.8	0	0.2262	-46	2.1923
	0.9	0	0.2272	-73	2.2694
		$\theta=0$		$\theta=0$	
10	0	0	1.5488	0	0.5879
	0.2	0	1.5487	0	0.5879
	0.5	0	1.5482	0	0.5878
	0.7	0	1.5463	0	0.5874
	0.8	0	1.5444	0	0.5870
	0.9	0 (-90)	1.5414 (-1.6973)	0	0.5864
		$\theta=0$		$\theta=0$	
10^5	0	0	1.6523	0	0.7081
	0.2	0	1.6523	0	0.7081
	0.5	0	1.6519	0	0.7079
	0.7	0	1.6502	0	0.7072
	0.8	1	1.6484	0	0.7065
	0.9	1 (-90)	1.6459 (-2.9225)	0 (-90)	0.7054 (-1.2785)

(3) When $E_I/E_M>1$, the interaction appears as a large compressive stress σ_n around $\psi=-\pi/2$ when $b/d>0.7$ (see Figs. 10-12). However, the maximum tensile stress σ_n near $\psi=0$, which may cause debonding the interface, is almost independent of the interaction. When $E_I/E_M<1$, the interaction appears as a large tensile stress σ_θ. When b/d and E_I/E_M are fixed, the interaction appears largely when a/b is large as shown in Figs. 10-15.

References

(1) Donnel, L.H., Stress Concentrations due to Elliptical Discontinuities in Plates under Edge Forces, Ann. Vol. T. Von Karman, Calif. Inst. Tech. (1941), p. 293-309.

(2) Shioya, S., Tension of a Infinite Thin Plate Having Two Equal Circular Inclusions, Trans. Jpn. Soc. Mech. Eng.,(in Japanese), Vol. 36 (1970), p. 886-897.

(3) Eshelby, J.D., The Determination of the Elastic Field of an Ellipsoidal Inclusion, and Related Problems, Proc. Royal Soc., A., Vol. 241 (1957), p. 376-396.

(4) Eshelby, J.D., The Elastic Field outside an Ellipsoidal Inclusion, Proc. Royal Soc., A., Vol. 252 (1959), p. 561-569.

(5) Noda N.A. and Matsuo, T., Analysis of a Row of Elliptical Inclusions in an Plate Using Singular Integral Equations, International Journal of Fracture, Vol. 83 (1997), p. 315-336.

(6) Edwards, R.H., Stress Concentrations around Spheroidal Inclusions and Cavities, Trans. ASME, J. Appl. Mech., Vol. 19, No. 1 (1952), p. 19-30.

(7) Eubanks, R.A., Stress Interference in Three-Dimensional Torsion, Trans. ASME, J. of Appl. Mech., Series E, Vol. 32, No. 1 (1965), p. 21-25.

(8) Shelly, J.F. and Yu, Yi-Yuan, The Effect of Two Rigid Spherical Inclusions on the Stresses in an Infinite Elastic Solid, Trans. ASME, J. of Appl. Mech., Series E, Vol. 33, No. 1 (1966), p. 68-74.

(9) Goree, J.G. and Wilson, H.B., Axisymmetric Torsional Stresses in a Solid Containing Two Partially Bonded Rigid Spherical Inclusions, Trans. ASME, J. of Appl. Mech., Series E, Vol. 34, No. 2 (1967), p. 313-320.

(10) Atsumi, A., Stresses in a Circular Cylinder Having an Infinite Row of Spherical Cavities Under Tension, Trans. ASME, J. of Appl. Mech., Series E, Vol. 27, No. 1 (1960), p. 87-92.

(11) Miyamoto, H., On the Problem of the Theory of Elasticity for a Region Containing more than Two Spherical Cavities (First Report, Theoretical Calculations), Trans. Jpn. Soc. Mech. Eng., (in Japanese), Vol. 23, No. 131 (1957), p. 431-436.

(12) Nisitani, H., Approximate Calculation Method of Interaction between Notches and Its Application, Journal of the JSME (in Japanese), Vol. 71, No. 589 (1968), p. 35-47.

(13) Nisitani, H., On the Tension of an Elastic Body Having an Infinite Row of Spheroidal Cavities, Trans. Jpn. Soc. Mech. Eng., (in Japanese), Vol. 29, No. 200 (1963), p. 765-768.

(14) Noda, N.A., Matsuo, T., Harada, S. and Nakamura, M., Singular Integral Equation Method in the Analysis of Interaction between Ellipsoidal Inclusions, Trans. Jpn. Soc. Mech. Eng., (in Japanese), Vol. 61, No. 585, A (1996), p. 1051-1058.

(15) Tuchida, E., Nakahara, I. and Kodama, M., Asymmetric Problem of Elastic Body Containing Several Spherical Cavities (First Report: Two Spherical Cavities in an Elastic Body), Trans. Jpn. Soc. Mech. Eng., (in Japanese), Vol. 42, No. 353 (1976), p. 46-54.

(16) Tuchida, E., Uchiyama, N., Nakahara, I. and Kodama, M., Asymmetric Problem of Elastic Body Containing Several Spherical Cavities (Second Report: Three Spherical Cavities in an Elastic Body), Trans. Jpn. Soc. Mech. Eng., (in Japanese), Vol. 44, No. 382 (1978), p. 1876-1883.

(17) Noda, N.A., Ogasawara, N. and Matsuo, T., Interaction Effect between Ellipsoidal Cavities in an Infinite Body under Uniaxial Tension, Trans. Jpn. Soc. Mech. Eng., (in Japanese), Vol. 62, No. 596, A (1996), p. 1051-1058.

(18) Noda, N.A., Ogasawara, N. and Matsuo, T.,

NII-Electronic Library Service

Interaction Effect among a Row of Ellipsoidal Cavities in an Infinite Body under Uniaxial Tension, Trans. Jpn. Soc. Mech. Eng., (in Japanese), Vol. 62, No. 602, A (1996), p. 2283-2289.

(19) Noguchi, H., Nisitani, H., Goto, H. and Mori, K., Semi-Infinite Body with a Semi-Ellipsoidal Pit under Tension, Trans. Jpn. Soc. Mech. Eng. (in Japanese), Vol. 53, No. 488 (1987), p. 820-826. [JSME International Journal Series I, Vol. 32, No. 1 (1989), p. 14-22]

(20) Noda, N.A. and Tomari, K., Fundamental Solution and its Application for Stress Analysis of Axisymmetrical Body under Asymmetric Uniaxial Tension, Bulletin of the Kyushu Institute of Technology, (in Japanese), Vol. 70 (1998), p. 7-12.

NII-Electronic Library Service